Toolpath Generation for 5-axis

Additive Manufacturing:

Effects of various 3D Printing Parameters on PLA FDM process

Project Supervisor: Charlie C.L. Wang

Student ID: 10683124

Jiahao Geng

University of Manchester

Department of Mechanical, Aerospace and Civil Engineering

2022-23

COPYRIGHT STATEMENT

i. Copyright in text of this dissertation rests with the author. Copies (by any process) either in full, or of extracts, may be made only in accordance with instructions given by the author. Details may be obtained from the appropriate Graduate Office. This page must form part of any such copies made. Further copies (by any process) of copies made in accordance with such instructions may not be made without the permission (in writing) of the author.

ii. The ownership of any intellectual property rights which may be described in this dissertation is vested in the University of Manchester, subject to any prior agreement to the contrary, and may not be made available for use by third parties without the written permission of the University, which will prescribe the terms and conditions of any such agreement.

iii. The ownership of any patents, designs, trademarks and any and all other intellectual property rights except for the Copyright (the "Intellectual Property Rights") and any reproductions of

copyright works, for example graphs and tables ("Reproductions"), which may be described in this thesis, may not be owned by the author and may be owned by third parties. Such Intellectual Property Rights and Reproductions cannot and must not be made available for use without the prior written permission of the owner(s) of the relevant Intellectual Property Rights and/or Reproductions.

iv. Further information on the conditions under which disclosures and exploitation may take place is available from the Head of the School of Mechanical, Aerospace and Civil Engineering (MACE).

DECLARATION

No portion of the work referred to in the dissertation has been submitted in support of an application for another degree or qualification of this or any other university or other institute of learning.

Acknowledgements

I would like to express my deepest gratitude and appreciation to my supervisor, Professor Charlie Wang, for his unwavering guidance, support, and mentorship throughout the course of my individual project.

I am also extremely grateful to Tianyu Zhang, a dedicated postgraduate student, who has generously shared his invaluable insights, experience, and time during the various stages of this project. His collaborative spirit and willingness to help have significantly contributed to the quality of my work and enhanced my understanding of the subject matter.

Finally, I would like to acknowledge the entire faculty and staff in our department for creating a stimulating and supportive academic environment that has fostered my development as a researcher and an individual.

Table of Contents

COPYRIGHT STATEMENT

DECLARATION

Acknowledgements

1. Abstract 8

2. Introduction 9

3. Literature Review 14

3.1. about 3-axis printing 14

3.2. 5-axis printing 18

4. Methodology 21

4.1. For 3-axis printing 21

4.2. For 5-axis printing 23

4.2.1. Slicing process 23

4.3.1. The Tool Length 26

4.3.2. The Z-coordinate 29

5. Result 34

5.1. For 3-axis Printing 34

6. Discussion 52

7. Conclusion 53

8. References 54

9. Appendix: A (not complete yet) 57

1. Abstract

Material extrusion is a commonly used technique in additive manufacturing, while 5-axis printing is a newer 3D printing method. Compared to traditional 3-axis printing, 5-axis printing has lots of advantages such as the reduced need for support structure and the ability of more complex and intricate geometries. However, its application in finished products is constrained by its error-proneness due to the complex movement and high requirements for precise control.

The objective for this project is to identify the printing parameters that would influence the result of the final 3D printing products and find feasible ways to improve it.

The tests were first taken on different printing parameter settings and the product dimensions were measured and compared to find out the effect of each parameter on the product. The study about 3-axis (planar) printing revealed that the precision of dimensions could be compromised by thicker layer sizes and faster printing speeds. This is because the thick layers of material tend to expand, while the high printing speeds hinder the precise placement of the printed material. Furthermore, the printing temperature, which affects the material's thickness, is also important in reducing the dimensional errors caused by thicker layers and faster printing speeds. Because the 5-axis printing tests in this study used the same material (PLA) as the tests of 3-axi printing, the result gained from the planner printing could be a guide for curved layer printing to some extent. For the 5-axis printing method, a calibration method will be introduced, and the tests mainly focused on the effect of printing patterns. The result shown that the contour pattern would be a better choice for curved layer because it has better surface quality and needs less time to generate toolpath and print.

2. Introduction

Since its inception in the 1980s, the field of additive manufacturing, often known as three-dimensional (3D) printing, has been seeing consistent growth. A computer-aided design (CAD) model is utilized in the process of creating pathways along which material is deposited layer-upon-layer consecutively in order to produce pieces. These days, additive manufacturing may make use of many different kinds of materials, ranging from rigid metals to pliable polymers. According to Gao (2015), the applications of additive manufacturing have expanded to include a wide variety of fields of study, ranging from large-scale architectural constructions to nanoscale bio-fabrication. The most common method of additive manufacturing (AM), known as fused deposition modelling (FDM) or fused filament fabrication (FFF), is dependent on the malleability of thermoplastics when they are heated to low temperatures. This allows for the deposition of liquid material in order to form the solid item. Even though it is primarily used for the production of prototype parts, fused deposition modelling (FDM) is significantly more cost-effective than other additive manufacturing processes, such as metal-specific selective laser sintering/melting (SLS/SLM) (Matsuzaki, 2017). According to Huang (2015), the lack of consistency and reliability in material qualities, as well as a lack of dimensional precision, is a barrier to the deployment of additive manufacturing in the rigorous environment of industrial production. In order for additive manufacturing to be able to satisfy more demanding applications, it is essential to remove the obstacles that are stopping technology from living up to its promise of ushering in a manufacturing revolution. The multi-axis AM(MAAM) concept can be broadened from the traditional uniaxial AM design to open up new research directions. In addition to the conventional relative motion that takes place along all three axes between the tool and the

workpiece, multi-axis systems include one or more additional directions of movement that make it possible to position the tool in a variety of different ways. Given that multi-axis manufacturing has already established itself in the machining sector as a result of extensive research and innovative uses in the production of complicated parts, the idea behind multi-axis manufacturing is not exactly groundbreaking. On the other hand, when it comes to AM, the research, hardware, and software that are now accessible in MAAM are inadequate, which necessitates an update of the facilities that are currently in place (Wulle, 2017). Major problems in additive manufacturing are mechanical strength and geometric precision of generated items. The stairstep (or staircase) phenomenon, which causes ridges the size of layer thickness on surfaces that are supposed to be smooth, has an impact on the surface quality of items made using additive manufacturing. The staircase effect also requires postprocessing steps like polishing in addition to form deviation (Cheng, 2011). In an analysis of top and side profile surface quality in FDM, mathematical models of surface deviations are investigated (Jin YA, 2015).

The concept of Curved Layer Fused Deposition (CLFD) modelling is incorporating the z-axis into the common 2D layer route of three-axis 3D printers (Chakraborty, 2008). The deposition path normal vectors for this technique's curved layer just slightly vary from vertical. Limited surface geometry and the potential for shearing and scraping during deposition are drawbacks of employing three-axis 3D printers for curved layers. While uniaxial deposition is used in literature's CLFD, problems such the need for a support structure and staircase effects (particularly on side surfaces) are still a major problem. As a result, the use of a 5-axis gantry is suitable for 3D printing using curved layers (Jin Y, 2017).

However, with 5-axis 3d printing, defects, inaccuracies, or other problems regarding the quality often arise (Spoerk,2019). In example, the surface roughness of items produced using 3D printing cannot compete with the quality of parts produced using traditional subtractive manufacturing processes or injection molding. Currently, the time, cost, and technological difficulties associated with postprocessing these surfaces outweigh the time and money saved by the more practical 3D printing process and limit FFF from being used in industry (Lalehpour, 2016). One way to mitigate these issues is to optimize the procedure ahead by choosing the right printing parameters (Valerga, 2019). Investigating the various individually changeable printing parameters and their randomized behaviors in the FFF printing process is important to achieve this.

The material that is frequently used for a variety of 3D printing applications is polylactic acid (PLA), a biodegradable material that is simple to print and has fewer printing issues with adhesion to the printing platform and the resulting warping of the part (Fernandes, 2018). A print issue occurs when the corners of the printed part bend up and separate from the build platform because there is insufficient adhesion between the printed part and the platform. Five process parameters (flow index, layer thickness, printing speed, printing temperature, and infill pattern) were examined in this work to determine their impacts and interactions on the produced surface roughness and dimensional accuracy.

The existing papers mainly discussed the printing parameter's effect on 3-axis (planar) 3D printing. Since 5-axis 3D printing is more complex, this project would investigate if these parameters had similar influences on the models produced by the 5-axis printer. By finding suitable parameter settings, the defects and inaccuracy

during 5-axis printing could be reduced, which also saves post-processing time and costs.

In the study, to determine the impact of each printing parameter on the final product, tests were first conducted using various printing parameter settings, and product dimensions were measured and compared. According to a study on 3-axis (planar) printing, thicker layer thicknesses and quicker printing rates may affect the accuracy of dimensions. This is due to the fact that thick layers of material have a tendency to expand, and fast printing speeds make it difficult to arrange printed material precisely. Additionally, the printing temperature, which has an impact on the thickness of the material, is crucial for minimizing the dimensional inaccuracies brought on by thicker layers and quicker printing rates.

An important hypothesis in this study is that the result gained from the planner printing could be a guide for curved layer printing to some extent because the 5-axis printing tests in this study used the same material (PLA) as the tests of 3-axi printing. A calibration technique will be introduced for the 5-axis printing method, with the major focus of the testing being the impact of printing patterns. The outcome demonstrated that the contour pattern would be a preferable option for curved layers because of its better surface quality and quicker toolpath generation and printing times. The result of this report could give some guidance for the future 5-axi printing works to improve the product quality. The limitation in this study is that the number of tests is constrained by the availability of 5-axi 3D printer, so the result could only represent a limit circumstance, for example, a simple curved layer instead of a complex wavy surface.

In general, the following report is organized into 5 main sections:

Literature Review: This section presents a comprehensive review of the existing literature related to the research topic, discussing key studies, theories, and gaps in the current body of knowledge.

Methodology: This section details the calibration method, research design, materials, procedures, and data analysis methods used in the study. It provides a clear and comprehensive account of the methods employed.

Results: This section presents the findings of the study, including data analysis, statistical results, and observed trends or patterns. It provides a clear and concise summary of the outcomes obtained from the research.

Discussion: This section interprets the results in the context of the research question and objectives, comparing the findings with existing literature and addressing any limitations or challenges encountered during the study. It discusses the implications of the results and suggests avenues for future research.

Conclusion: This section summarizes the key points of the report, including the research question, objectives, methods, results, and their implications. It highlights the significance of the study, offers recommendations for future research or practice.

3. Literature Review

3.1. about 3-axis printing

Griffiths et al. (2016) conducted an experiment to investigate the effects of altering four process factors - slice orientation, infill percentage, number of shells, and layer thickness - on the amount of waste generated throughout the 3D printing process. The study found that slice orientation had the most significant impact on scrap weight, while layer thickness played a crucial role in determining the manufacturing time. Furthermore, the researchers highlighted the trade-offs between production time and material waste when changing the slice orientation. These effects were not mutually exclusive, as the orientation resulting in a larger vertical cross-sectional area led to more waste but fewer layers and a shorter production time.

This research offers valuable insights into the significant impact of slice orientation on waste generation during the 3D printing process, suggesting the importance of carefully adjusting this parameter when optimizing 3D printing settings. Doing so could lead to reduced material waste and improved production efficiency in practical applications. However, the study did not address the critical factor of nozzle temperature, which can influence the melting and cooling rates during 3D printing and, consequently, affect the final print quality. Future research could benefit from incorporating nozzle temperature along with the other parameters to further optimize the 3D printing process.

Ehsanul Haque et al. (2019) introduced a novel approach by employing a design of experiments (DOE) called the face-centered central-composite design (FCCCD), which effectively reduced the total number of experiments required. This method utilized various altering parameters such as layer thickness, overlap distance, raster

width, and part orientation to design the specimens and measure the surface roughness. Moreover, the specimens were designed using a randomized part orientation. The findings indicated that layer thickness was the most influential parameter for improving the surface finish.

This research has its merits, such as the introduction of a new experimental method that effectively reduces the number of experiments needed, which can save time and resources. However, there are some limitations to this study as well. For instance, it focused solely on surface roughness and did not consider dimensional accuracy, which is also a critical factor in evaluating 3D-printed parts' overall quality. Additionally, the study lacks an investigation into the influence of temperature, which can play a significant role in determining the final quality of printed objects. Future research could address these limitations by examining the impacts of both dimensional accuracy and temperature on the 3D printing process, leading to a more comprehensive understanding of the optimization of 3D printing parameters.

Pérez et al. (2018) conducted a study to examine the effects of layer thickness, printing speed, temperature, and wall thickness on surface roughness in 3D printing. By employing analysis of variance (ANOVA), the researchers demonstrated that layer thickness and wall thickness were crucial parameters, while printing speed and temperature seemed to have a less significant impact.

This research has its strengths, such as the use of ANOVA, which provides a clear and intuitive representation of the influence of different factors on surface roughness. This method allows for a better understanding of the relative importance of each parameter in the 3D printing process. However, there are also limitations to this study. One notable drawback is the exclusive focus on surface roughness, without

considering the equally important factor of dimensional accuracy, which is essential for assessing the overall quality of 3D-printed parts. Moreover, the study did not investigate the influence of slicing orientation, which, as demonstrated by previous research, can have a significant impact on the final print quality. Future studies could address these limitations by including dimensional accuracy and slicing orientation in their analysis, leading to a more comprehensive understanding of the factors that contribute to the optimization of 3D printing parameters.

Valerga et al. (2018) conducted a study to explore the effects of material pigmentation, environmental humidity, and extrusion temperature on the surface quality, dimensional quality, and mechanical strength of 3D-printed parts. The results showed that extrusion temperature played a significant role in influencing surface and dimensional attributes. It was found that increasing the extrusion temperature led to a decrease in the material's viscosity, which in turn resulted in greater dimension variation. Additionally, a higher extrusion temperature contributed to the formation of bubbles, adversely affecting surface quality and increasing dimensional deviations.

This research has its merits, such as considering the impact of environmental humidity, which is an often-overlooked factor that can affect 3D printing outcomes. By incorporating this variable, the study provides a more comprehensive understanding of the factors influencing 3D printing quality. However, there are limitations to this study as well. One notable drawback is the narrow focus on temperature as the primary factor affecting the printing process, while other potentially important factors such as printing speed, layer thickness, and slicing orientation were not considered. Future research could address these limitations by investigating a wider range of factors to gain a more holistic understanding of the optimization of 3D printing parameters.

Yang et al. (2019) investigated the effect that five printing settings had on the manufacturing time as well as the mechanical characteristics and surface finish quality of additively printed PLA test pieces utilizing FFF. They investigated how the surface roughness, tensile strength, and production time were affected by the nozzle diameter, liquefier temperature, extrusion rate, filling velocity, and layer thickness, each of which had three levels to choose from. They verified the previously constructed regression model by doing the experiment using a central composite design, and they demonstrated that raising the nozzle diameter, filling velocity, and layer thickness resulted to increases in surface roughness and tensile strength, while simultaneously reducing the amount of time needed for production. In general, the temperature of the liquefier and the extrusion velocity had less influence on the product than was anticipated.

Brion et al. (2021) demonstrated that training a multi-head neural network using images annotated in terms of departure from ideal printing parameters enables robust and generalizable real-time extrusion AM error detection and rapid correction. This was accomplished by using images marked in terms of the amount of divergence from the optimal printing parameters. The automation of data acquisitions as well as labelling makes it possible to generate a training image-based dataset that is sufficiently vast and diverse to enable error identification and correction that is applicable to actual 2D and 3D geometries, materials, printers, toolpaths, and even extrusion methods. This was made possible by the automation of both data acquisition and labelling. From the images of the nozzle that were taken while printing, the deep multi-head neural network was able to simultaneously and with a high degree of accuracy forecast the four most important printing parameters: flow rate, lateral speed, Z offset, and extrusion temperature. Alongside this network, numerous

advancements were presented in the feedback control loop with new additions such as proportional parameter updates, toolpath splitting, and optimized prediction thresholding. These new additions, when combined, provide an order of magnitude improvement in correction speed and response time compared to previous work. However, transferring the algorithm from 3-axis to 5-axis printing is very difficult. The complexity of motion for 5-axis printing is much higher than 3-axis, so the number of images needed for network training might be too numerous.

3.2. 5-axis printing

Singamneni et al. (2012) demonstrated the usefulness of their four-vectors curved layer slicing algorithms by applying them to a variety of problems ranging in the degree of geometrical complexity they presented. It has been determined that Curved Layer Fused Deposition Modelling (CLFDM) can be effectively executed. According to the findings of the experiments, the mechanical performance of the items created using curved layer FDM is superior. When subjected to three-point bending, the average fracture compressive load of curved layer parts saw an approximately 40% increase in comparison to that of the flat layer counter parts. In spite of the fact that this may be attributed to the enhanced mesostructured, fracture zones unequivocally revealed that the structural integrity had been improved as a direct result of continuous fibers produced by CLFDM.

Zhang et al. (2021) presented a sampling-based motion planning method to solve the problems of singularity and collision in an integrated way to support the manufacturing realization of designed toolpaths for Multi-Axis Additive Manufacturing (MAAM) in various machine configurations. This method was developed to solve the problems of singularity and collision in an effort to

manufacture designed toolpaths. When necessary, variants with altered orientations are created for waypoints, and the optimal trajectory is determined by linking the IK solutions with the least amount of total angle change on the B- and C-axes. As a consequence of this, the quality of manufacturing may unquestionably be enhanced by optimizing for singularity, as has been established by experimental experiments.

Fang et al. (2020) presented a field-based methodology to calculate curved layers and toolpaths by extracting the iso-surfaces and iso-curves from the controlling scalar-fields. These are then optimized according to both the requirement of mechanical strength and the limits of manufacturing. In order to simplify the computation of optimization, they select an optimized vector-field to serve as an indication of the governing field's gradients. The normalized vector fields are then used to compute the final scalar-fields. With the use of this tactic, a nonlinear optimization problem can be broken down into several linear optimization problems, each of which can be addressed in an efficient and productive manner. It is possible to produce curved layers for supporting structures by extrapolating the controlling field into the regions that require support. In addition to this, algorithms are developed in order to ensure accessibility and manage the variance in layer thickness. The outcomes of the experimental testing provide grounds for a great deal of optimism. When compared to models generated using plane-based FDM, the models fabricated using the approach have a load-bearing capacity of 1.42–6.35 times greater.

Zhang et al. (2022) presented a new universal slicing framework for multi-axis 3D printing. In this framework, curved layers for material accumulation are formed in order to fulfill the combined objectives of support-free (SF), strength reinforcement

(SR), and enhanced surface quality (SQ) simultaneously on the same model. The entire framework is comprised of an inner loop of quaternion-field optimization and an outer loop of scale-controlled deformation, and both of them can be efficiently computed by local/global solvers.

In summary, the existing literature on 5-axis 3D printing predominantly focuses on the impact of algorithms for curved layer slicing and toolpath generation, while research on 3-axis 3D printing primarily investigates the effects of various printing parameters on aspects such as surface quality, dimensional accuracy, and mechanical strength. There is potential for further exploration of the influence of these parameters on 5-axis 3D printing. Consequently, this project aims to examine the relationship between different printing parameters and their effects on both 5-axis and 3-axis 3D printing processes. The results from this investigation will provide valuable insights for parameter settings in 5-axis 3D printing, thereby contributing to the optimization of this technology.

4. Methodology

4.1. For 3-axis printing

To analysis the effects of different printing parameters on the surface quality and dimension accuracy, a thin and flat model (30*30*2 mm) was created using Solidworks. The assumption here is that the performance for both planar and curved layers would be same when using the same material (PLA).

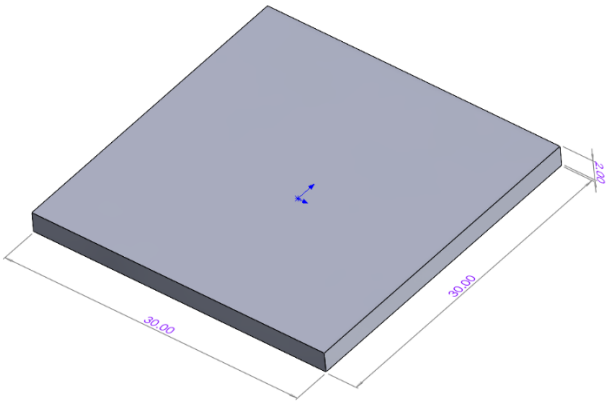

Figure 1 model with dimensions in Solidworks

Then, the model was imported into Cura to slice and generate toolpath under different printing parameter settings. The G-code will output automatically.

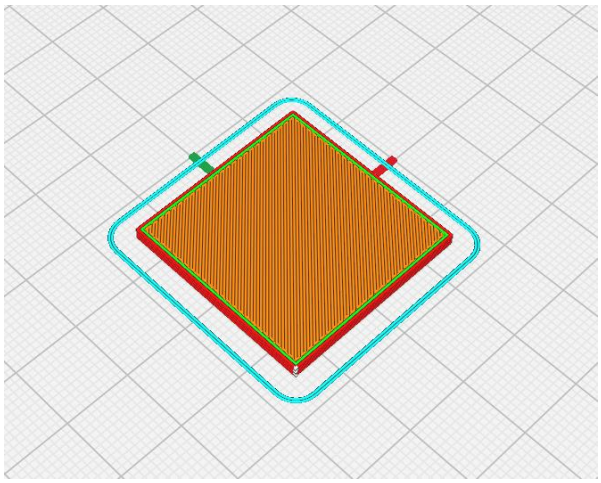

Figure 2 Preview with toolpath in Cura

The G-codes were imported to the Flsun Q5 3D printer to print the corresponding models. And choosing this machine was because of its usability.

Flsun Q5 – flsun3d

Figure 3 photo of *Flsun Q5 3D printer* from official website

In this experimental design, it aims to investigate the effects of five different parameters on the 3D printing process, which are Temperature, Flow index, Printing Speed, Layer Thickness and Infill Pattern. Initially, a default parameter combination was established, and each parameter was tested using five distinct values (pattern for 3). To control variables, all other parameters are kept constant during each test. For each trial, measure the length, height, and surface roughness of the printed object. By comparing these measurements to the computer model, we can determine the percentage error for each outcome. This approach allows us to systematically examine the impact of each parameter on the 3D printing process and draw insights from the results.

4.2. For 5-axis printing

4.2.1. Slicing process

Curved layer is the best way to show the characteristic of 5-axis 3D printing method. So, a dome shape model was created using Solidworks.

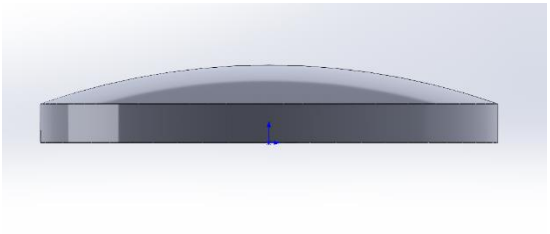

Figure 4 dome shape model in Solidworks

The model was then sliced using the program 'S3_DeformFDM' from Tianyu Zhang.

GitHub - zhangty019/S3_DeformFDM: S^3-Slicer: A General Slicing Framework for Multi-Axis 3D Printing

For the curved layer printed by 5-axis 3D printing method, the project would mainly focus on the surface quality, since the dimension accuracy is difficult to measure using conventional equipment. As a result, only the top surface layer was printed to simplify the experiment to save time. The rest part of the model was printed in planar to be used as the base.

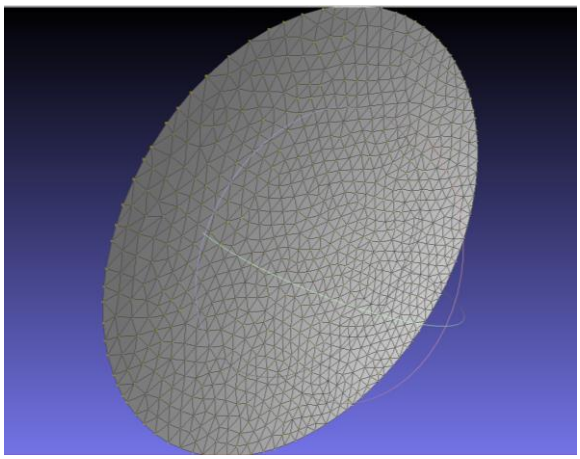

Figure 5 The view of mesh of the top layer in Meshlab

4.2.2. Toolpath generation process

The toolpaths of the curved layer were generated by the program ‘Toolpath_Gcode_generation’.

[zhangty019/Toolpath_Gcode_generation: Simple example which contains the different toolpath generation, and G-code generation for the 5AXISMAKER machine (github.com)]

The program allows users to choose one from three kinds of toolpath pattern, which are ‘Contour’, ‘Spiral’ and ‘Zigzag’.

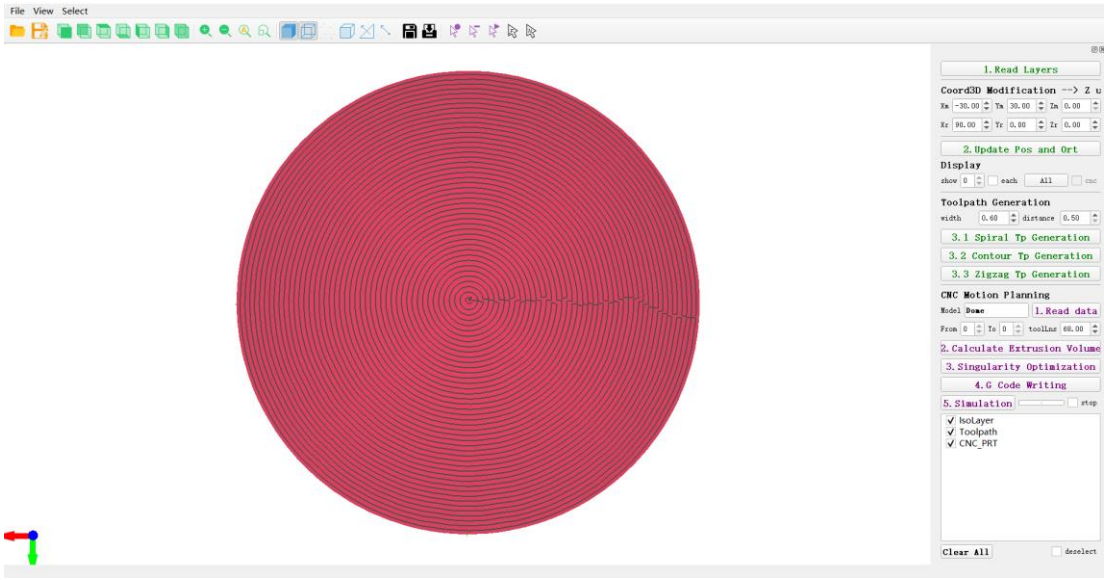

Figure 6 User window of the Toolpath_Gcode_generation program

The experiments were taken under 3 different patterns, with different temperatures and Flow index (Extrusion ratio). The results were used to compare and find the suitable setting.

```
    //inner parameters
    int m_jump_detection_threshold = 4.0;
    int Core = 16;
    int layerNum = 40;    // The number of detected bottom layer for height calculation
    bool is_planar_printing = false; //switch for the planar printing
    double ratio = 0.49;  // extrusion ratio
};
```

Figure 7 C++ code that sets the extrusion ratio.

4.3. Machine Calibration method

Basically, only the 5-axis 3D printer needs to be calibrated manually, the printer used in this project is from 5axismaker.

5XM Overview — 5AXISMAKER

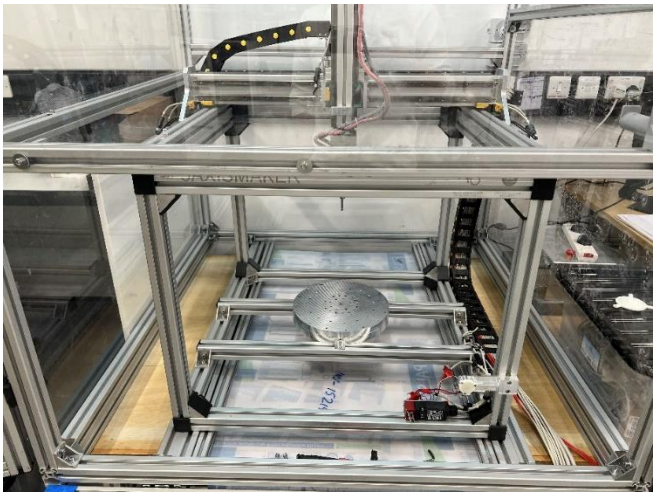

Figure 8 Photo of the 5-axis printer

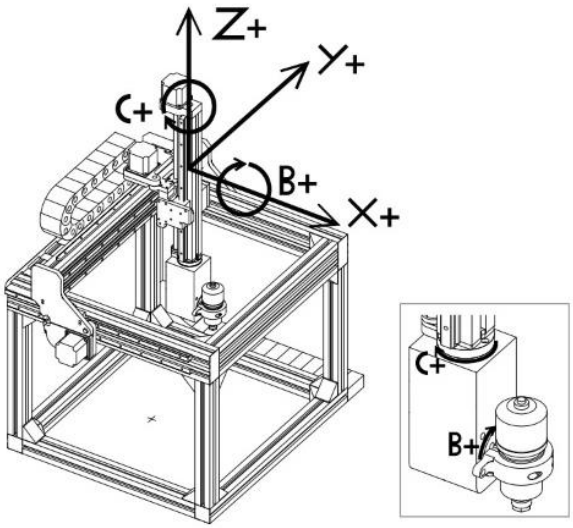

Figure 9 Axis Direction and Coordinates System, from official website

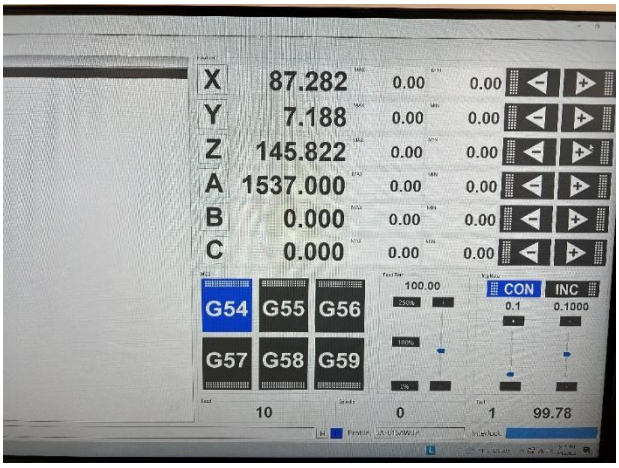

Figure 10 user interface window of the 5-axis printer

Because of the complex motion for the 5-axis 3D printer, it is very important to calibrate the machine before printing.

4.3.1. The Tool Length

Firstly, the tool length needs to be decided using the Dial Indicator. Because the extruder needs to rotate about the B-axis (Figure 4.3.2), it is crucial to get the accurate tool length to ensure that the motion planning for printing is correct.

Figure 11 the Dial Indicator with a magnetic stand

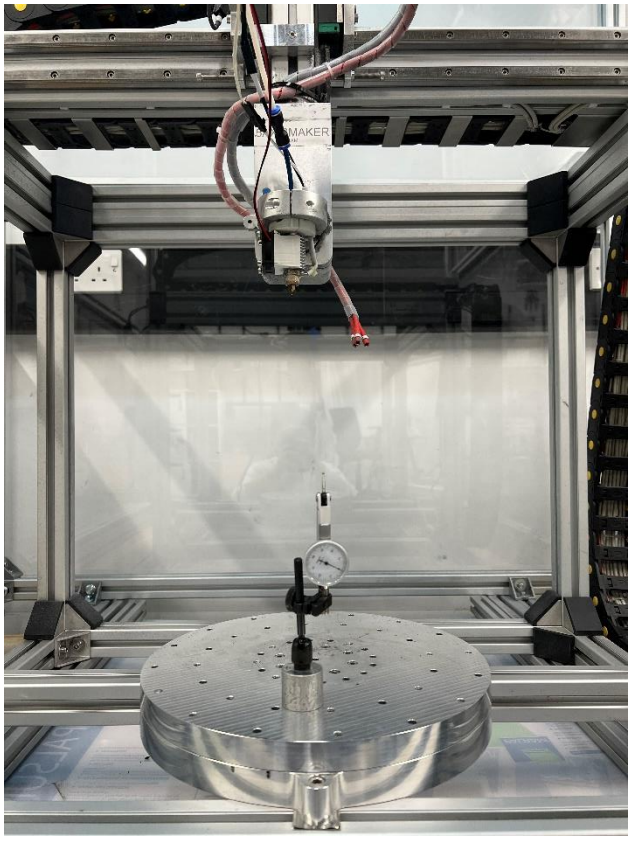

Figure 12 photo of how to place *the Dial Indicator* under the extruder.

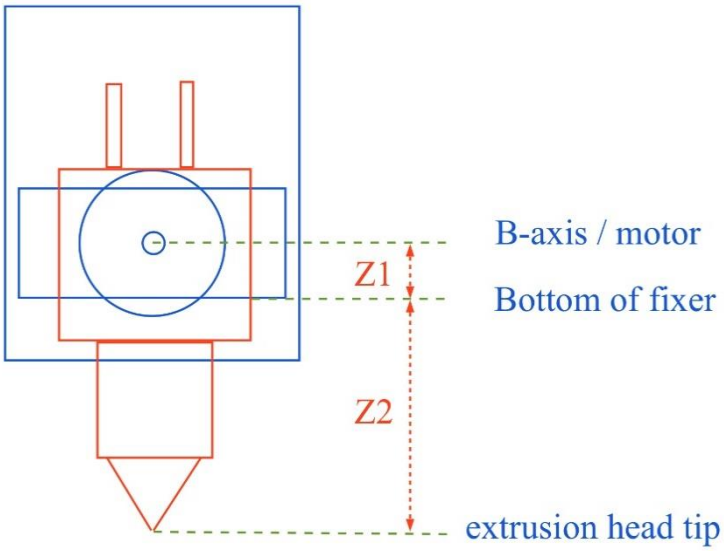

Figure 13 diagram shows how to decide the tool length.

The process of deciding the tool length is as following:

First, place the indicator as shown in Figure 12, then move the extruder until its tip just touch the indicator tip, the indicator would rotate a little bit, then record the Z-coordinate shown in the user window Figure 10. In this experiment, it was 165.175 mm.

Next, move the extruder and let its tip just touch the bottom of the fixer, the indicator would rotate a little bit, then record the Z- coordinate shown in the user window Figure 10. In this experiment, it was 107.192 mm.

Let 165.175 minus 107.182 to get Z_2 Figure 13. Because the value of Z_1 is given from the machine manual, which is 10 mm, the tool length is Z_1 + Z_2, which is 67.98 mm.

Figure 14 The extruder tip and small cylinder.

4.3.2. The Z-coordinate

To calibrate the Z-axis position, we need a pre-prepared small metal cylinder with an M6 size (Outer diameter of 6mm). During the calibration process, lower the printer's extruder head slowly while continuously rolling the cylinder back and forth under the extruder head using a pair of tweezers. Adjust the position until the distance between the extruder head and the base plate just allows the cylinder to pass through, as the Figure 14 shown above. At this point, set the Z-axis value to 6mm on the user interface to complete the calibration.

4.3.3. The XY-coordinates

To calibrate the X and Y axis position, first print a square with the current origin as the centre, then rotate the base plate 180 degrees and print another square with the same side length. If the two squares do not overlap, it indicates that the current origin is not on the Z-axis, which serves as the rotation axis, and there is a deviation from the actual origin, as shown in the Figure 15.

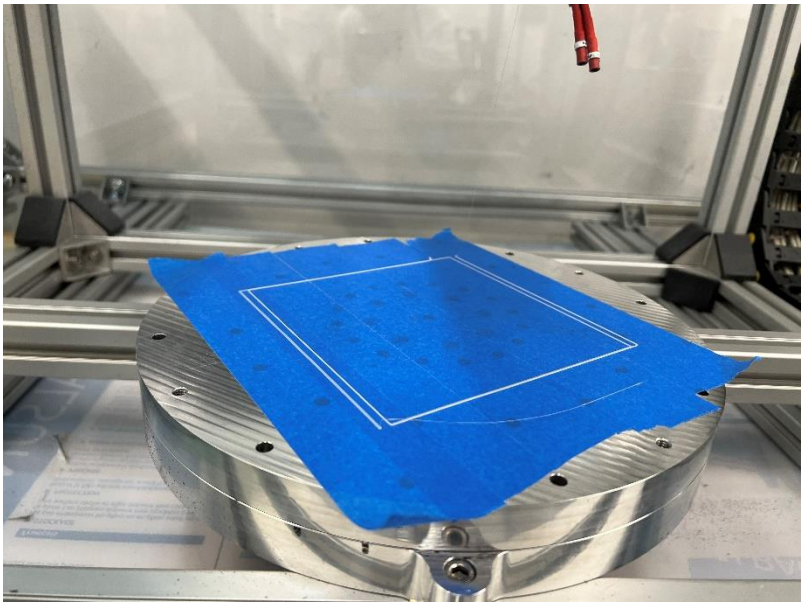

Figure 15 Photo of the squares for XY-axis calibration

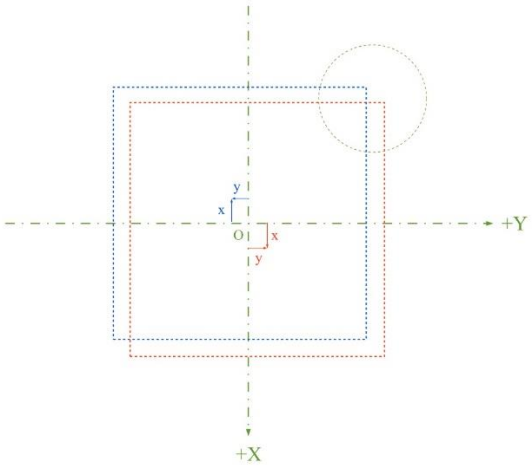

Figure 16 The diagram represents the deviations of XY-axis.

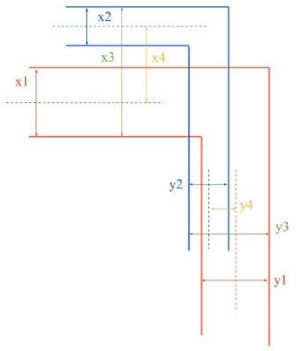

Figure 17 Details of the filament overlap at the corner.

As the Figure 16and Figure 17 shown above,

the deviation along X-axis can be found by: $\Delta X = \frac{X_4}{2} = (X_3 + \frac{X_1}{2} + \frac{X_2}{2})/2$

And deviation along Y-axis can be found by: $\Delta Y = \frac{Y_4}{2} = (Y_3 + \frac{Y_1}{2} + \frac{Y_2}{2})/2$

The values were measured by vernier calliper.

Input the calculated value for the XY-axis in the user interface to complete calibration.

4.4. Measurements of Dimensions

Dimension measurements are mainly taken for the planar models using vernier caliper as shown in Figure 18.

Figure 18 Measuring the side length using Vernier Calliper

In order to measure the side length and thickness of a 3D-printed square thin plate and calculate the percentage error, an experimental procedure was designed as follows. First, a caliper was used to measure the side length and thickness at three separate positions on the plate, with the readings recorded. The average side length and thickness were then calculated by summing the respective measurements and dividing the results by three. By comparing these average values with the corresponding dimensions from the original 3D model, percentage errors were calculated for side length and thickness. The recorded percentage errors for the side length and thickness served as an evaluation of the accuracy of the 3D-printing process.

4.5. Measurements of Surface roughness

The surface roughness is measured for both 3-axis and 5-axis printed models. A contact profilometer is selected and calibrated according to the manufacturer's guidelines to provide accurate and reliable measurements, shown in Figure 19. To obtain a comprehensive assessment of the overall roughness, 5 measurements were taken on different locations of the sample. The profilometer is carefully positioned at each location, and surface roughness data is collected, with a focus on the Ra value. Ra is the universally recognized, and most used, international parameter of roughness. It is the arithmetic mean of the absolute departures of the roughness profile from the mean line. After gathering the data, the average Ra value is calculated to represent the overall surface roughness of the 3D-printed sample. The results are then documented in a data table, including the average Ra value and the corresponding printing settings.

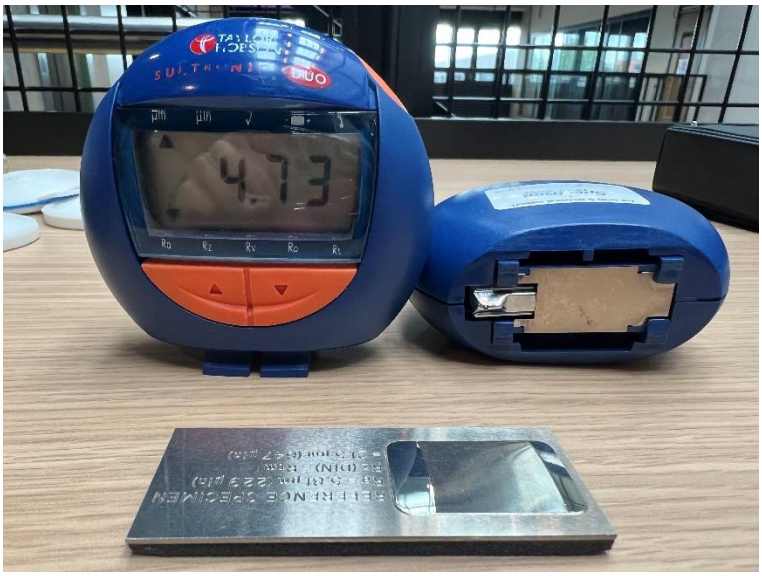

Figure 19 The contact profilometer used to measure the surface roughness.

4.6. Data Analysis Method

To analysis the collected data, firstly is organizing the data in a structured table, with columns representing the different parameters and output variables. Then, calculate the mean percentage error for sides and thickness, and the mean surface roughness for each parameter setting.

Plot the graphs based on the calculated data to show the general trend of effect of different printing parameters.

Apply the linear regression method to analysis the effects of different parameters on the 3D printing process and discover how these parameters influence the output variables. By fitting a multiple linear regression model to the data, with the output variable as the dependent variable and the input parameters as independent variables, it is able to estimate the magnitude and direction of each parameter's effect on the outcome. This analysis could help identify statistically significant parameters that have a meaningful impact on the 3D printing process, as indicated by low p-values. Additionally, the R-squared value obtained from the linear regression model represents the proportion of variance in the output variable that can be explained by the input parameters, offering a measure of the model's explanatory power. Through this approach, we can better understand the relationships between the parameters and the 3D printing process, enabling us to optimize and enhance the quality of the printed objects by adjusting the most influential parameters accordingly.

5. Result

5.1. For 3-axis Printing

To practice the method of controlling variables, firstly a default parameters setting is decided as the Base model.

Temperature: 200 °C.

Flow Index (α): 100 %

Printing Speed: 100 mm/s.

Layer Height: 0.3 mm

Infill Pattern: Zigzag

Figure 20 Base model

5.1.1. Effects of Temperature

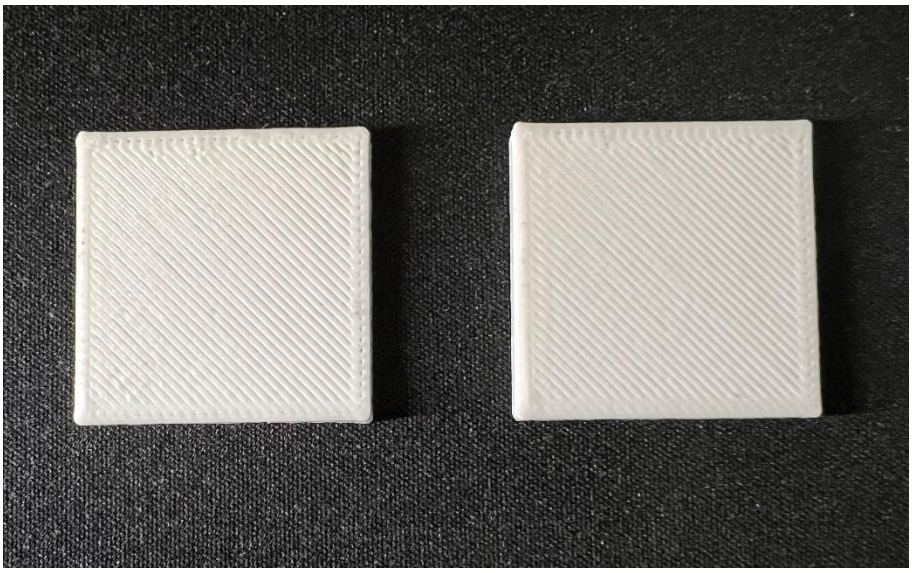

Figure 21 Temperature of 180℃ and 190℃

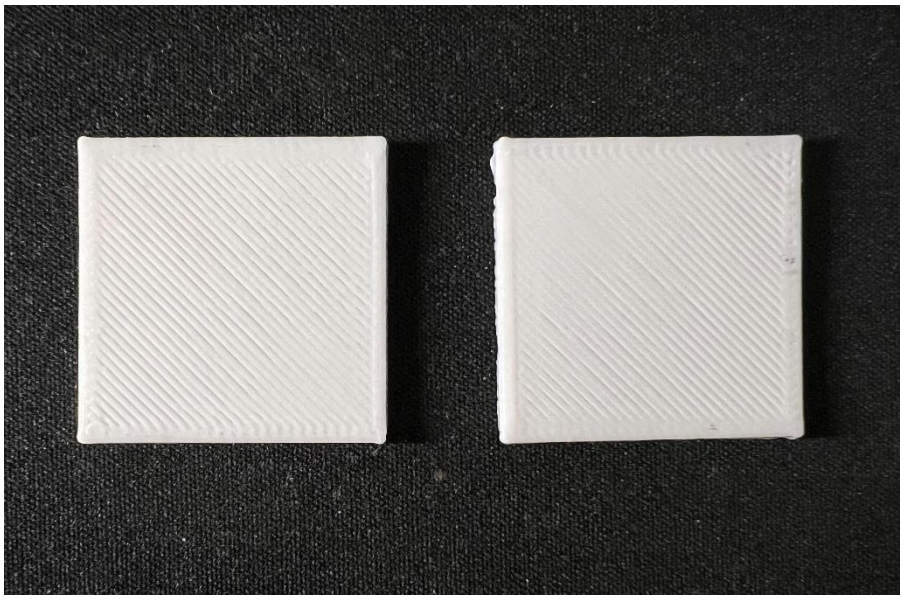

Figure 22 Temperature of 210°C and 220°C

	Table 1 - Temperature (°C)				
	180	190	200	210	220
Side Length (mm)	30.22	30.07	29.98	30.23	30.32
	30.18	30.11	30.01	30.16	30.26
	30.21	30.15	29.96	30.17	30.31
	30.18	30.23	30.01	30.29	30.26
	30.07	30.25	30.05	30.26	30.20
	30.09	30.31	30.04	30.23	30.21
% Error	0.53%	0.62%	0.03%	0.74%	0.87%
Thickness (mm)	2.01	2.03	1.98	2.07	2.05
	1.99	2.05	1.97	2.08	2.03
	2.02	2.04	2.01	2.06	2.06
% Error	0.33%	2.00%	-0.67%	3.50%	2.33%
Surface roughness (µm)	23.16	15.67	23.58	12.3	15.85
	21.06	19.05	19.57	21.53	13.12
	15.39	29.09	18.7	25.16	26.33
	24.04	25.86	11.21	16.69	25.58
	23.63	20.94	18.81	21.69	16.18
Average	21.456	22.122	18.374	19.474	19.412

Figure 23 Table for different Temperature settings

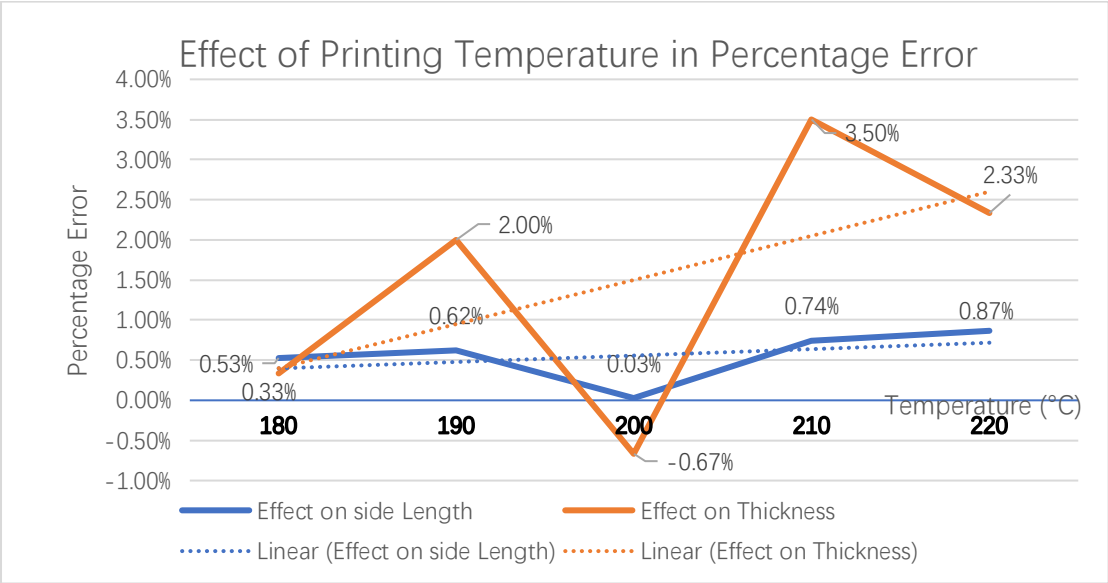

Figure 24 Effect of Printing Temperature in Percentage Error

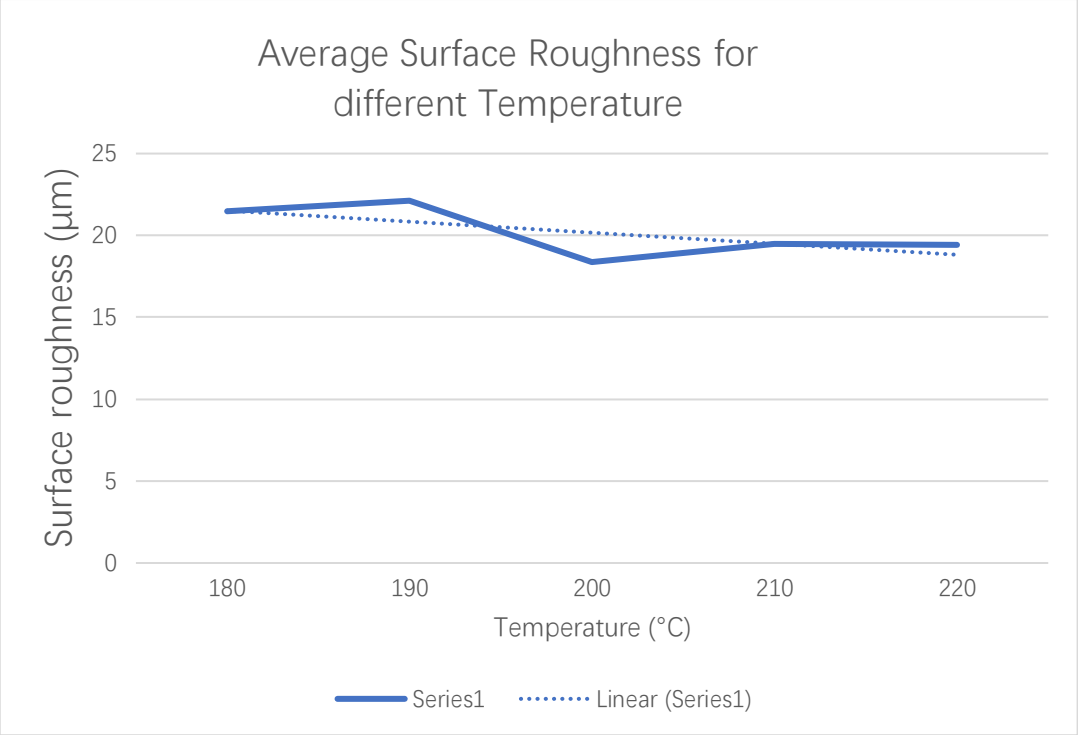

Figure 25 Effect of Printing Temperature in surface roughness

Basically, higher temperature would cause more percentage error on thickness but lower surface roughness

5.1.2. Effects of Flow Index

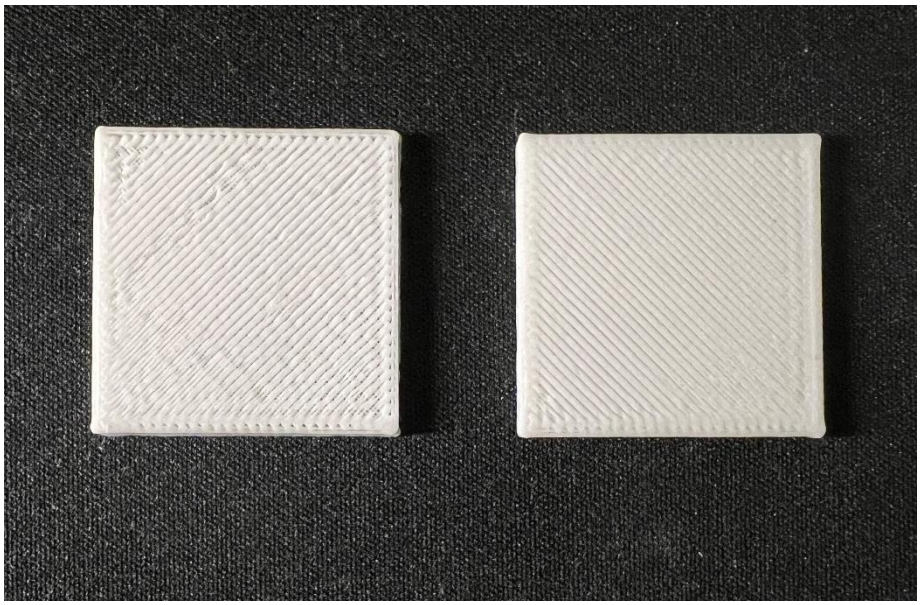

Figure 26Flow index of 60% and 80%

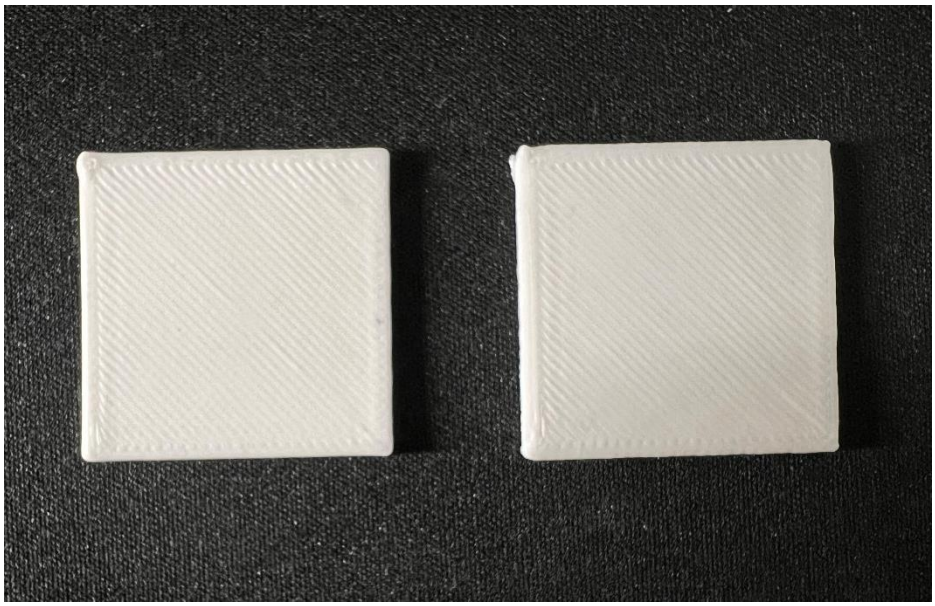

Figure 27 Flow index of 120% and 140%

	Table 2 - Flow Index (α) (%)				
	60	80	100	120	140
Side Length (mm)	29.94	29.85	29.98	30.17	30.53
	29.85	29.90	30.01	30.16	30.61
	29.95	29.94	29.96	30.12	30.66
	29.78	30.05	30.01	30.26	30.71
	29.84	30.13	30.05	30.28	30.74
	29.81	30.03	30.04	30.27	30.80
% Error	-0.46%	-0.06%	0.03%	1%	2%
Thickness (mm)	1.96	2.05	1.98	2.05	2.03
	1.94	2.01	1.97	2.07	2.01
	1.97	2.03	2.01	2.04	2.02
% Error	-2.17%	1.50%	-0.67%	2.67%	1.00%
Surface roughness (µm)	32.04	29.93	26.84	18.75	90.55
	31.32	30.51	25.61	14.13	5.19
	34.01	26.9	29.23	12.94	10.88
	29.86	24.15	15.31	15.26	1.71
	32.07	28.6	21.97	18.98	8.07
Average	31.86	28.018	23.792	16.012	23.28

Figure 28 Table for different flow index settings

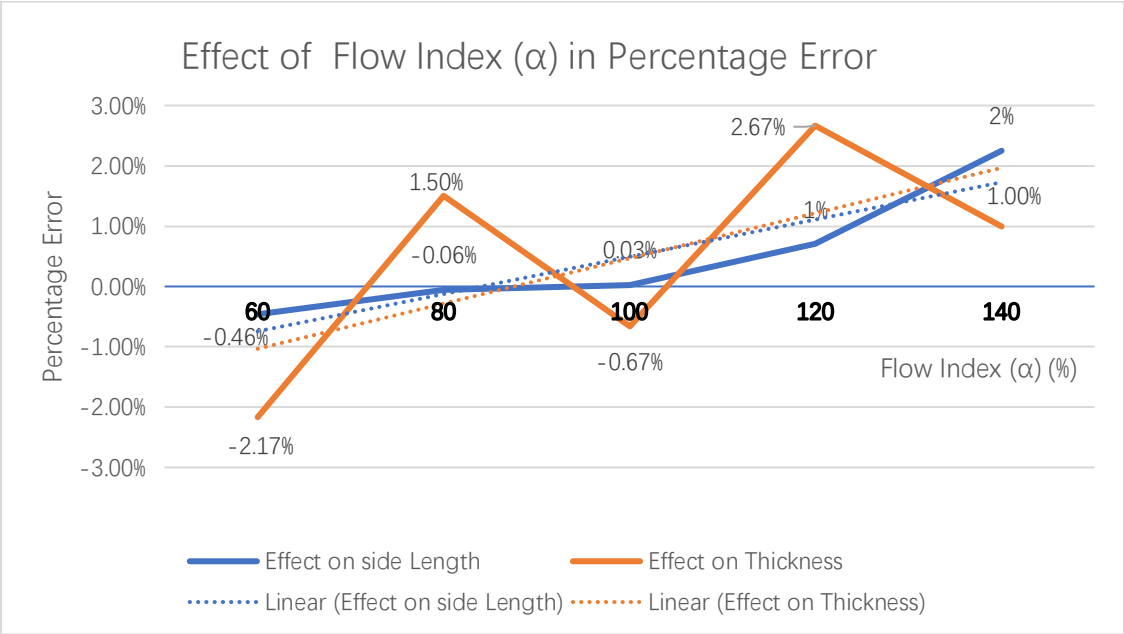

Figure 29 Effect of flow index in Percentage Error

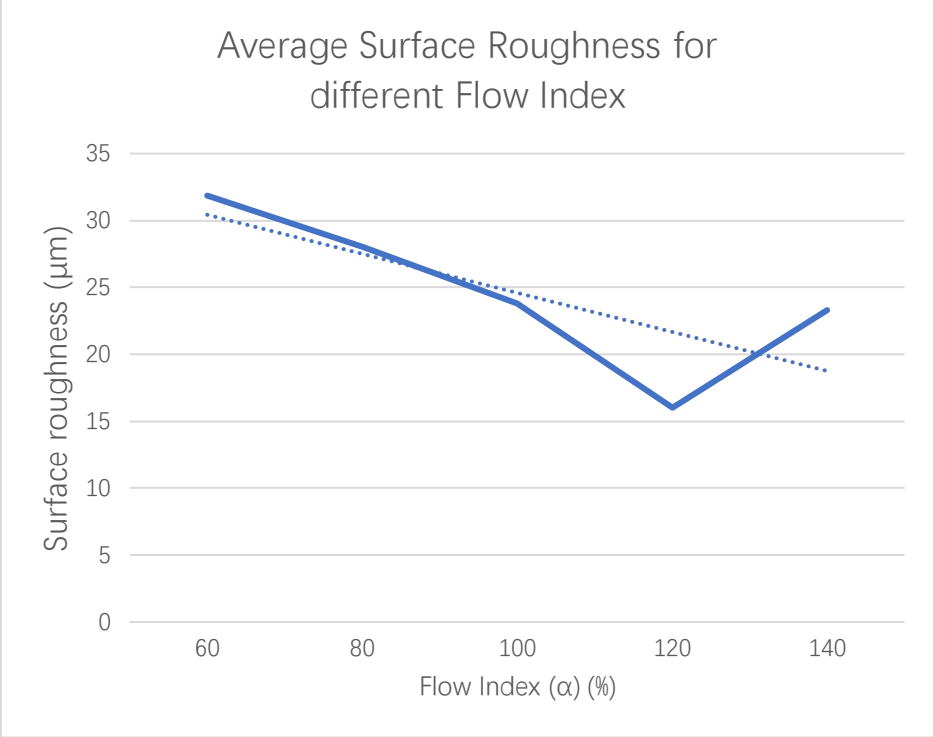

Figure 30 Effect of flow index in surface roughness

In general, higher Flow index would cause higher percentage error for both side length and thickness, but lower surface roughness.

5.1.3. Effects of Printing Speed

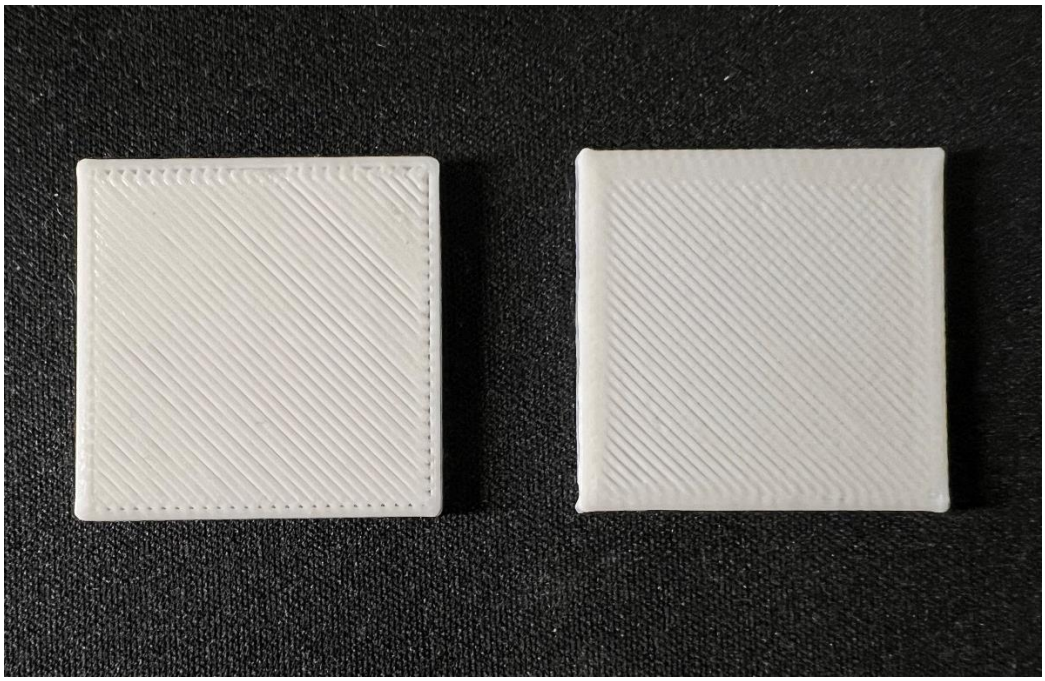

Figure 31 Printing speed of 30 mm/s and 90 mm/s

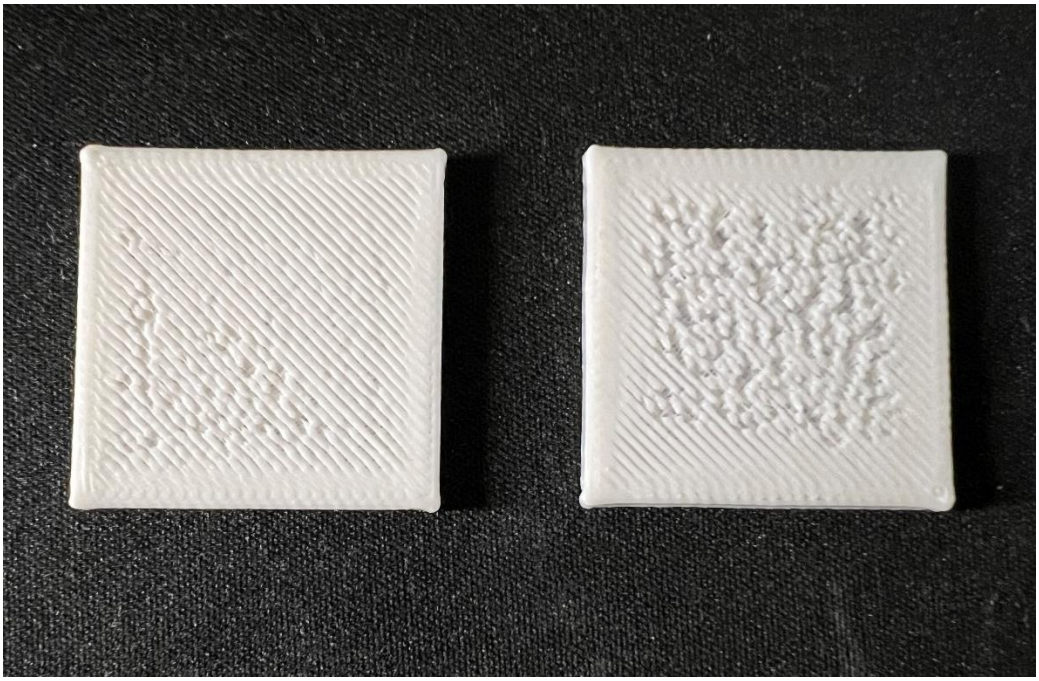

Figure 32 Printing speed of 120 mm/s and 150 mm/s

	Table 3 - Printing Speed (mm/s)				
	30	60	90	120	150
Side Length (mm)	30.06	29.98	30.29	30.18	30.22
	30.08	30.01	30.30	30.23	30.19
	30.11	29.96	30.27	30.21	30.26
	30.16	30.01	30.16	30.22	30.07
	30.14	30.05	30.22	30.25	30.09
	30.11	30.04	30.18	30.23	30.08
% Error	0.37%	0.03%	0.79%	0.73%	0.51%
Thickness (mm)	2.01	1.98	2.02	2.09	2.03
	2.03	1.97	2.01	2.08	2.07
	1.99	2.01	1.99	2.06	2.05
% Error	0.50%	-0.67%	0.33%	3.83%	2.50%
Surface roughness (µm)	19.55	26.84	4.78	9.81	31.49
	5.28	25.61	32.85	32.61	19.78
	19.74	29.23	8.47	10.71	23.19
	7.06	15.31	24.36	23.72	14.02
	17.55	21.97	28.17	32.36	32.82
Average	13.836	23.792	19.726	21.842	24.26

Figure 33 Table for different printing speed settings

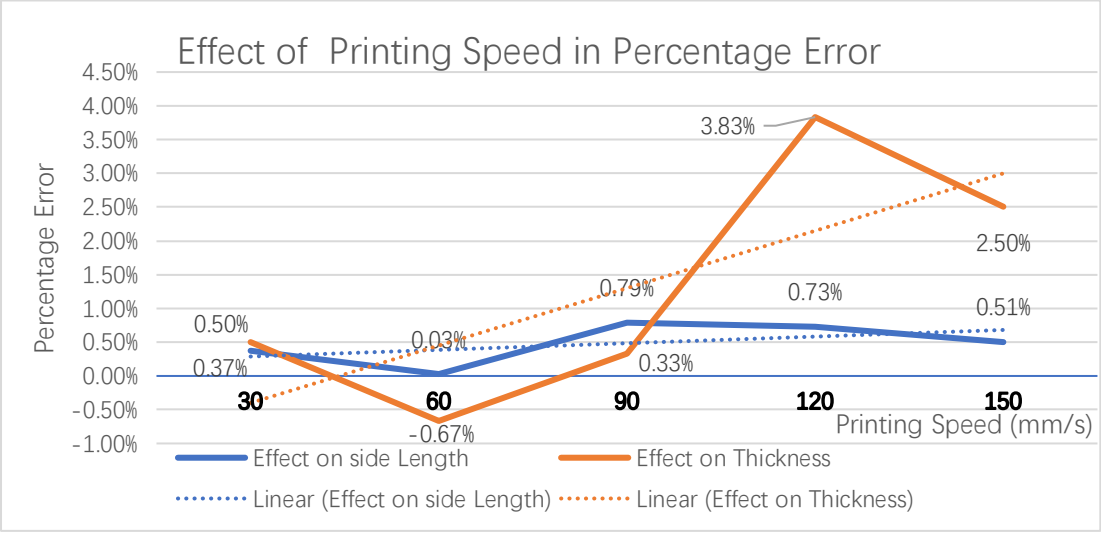

Figure 34 Effect of printing speed in Percentage Error

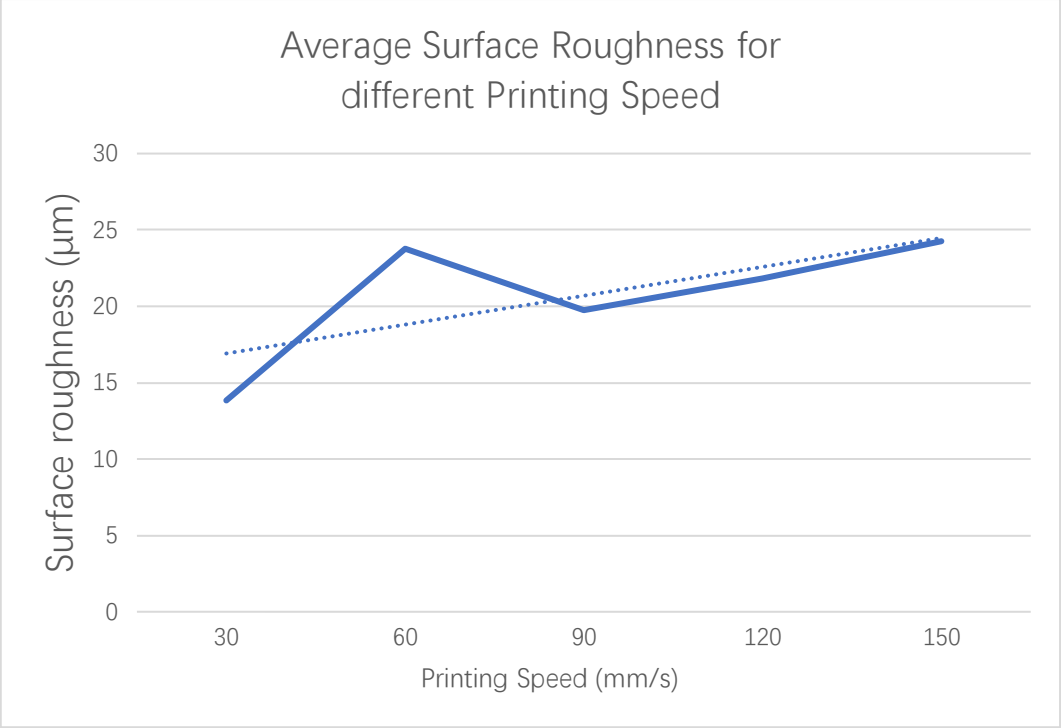

Figure 35 Effect of printing speed in surface roughness

Basically, higher Printing speed would cause more percentage error on thickness and higher surface roughness.

5.1.4. Effects of Layer height

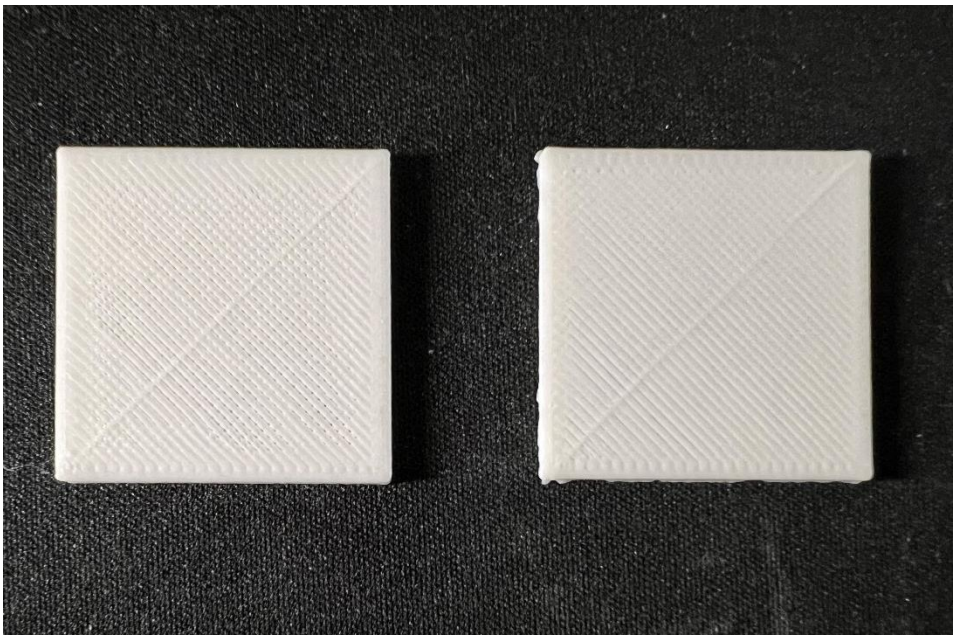

Figure 36 layer thickness of 0.15 and o.2 mm

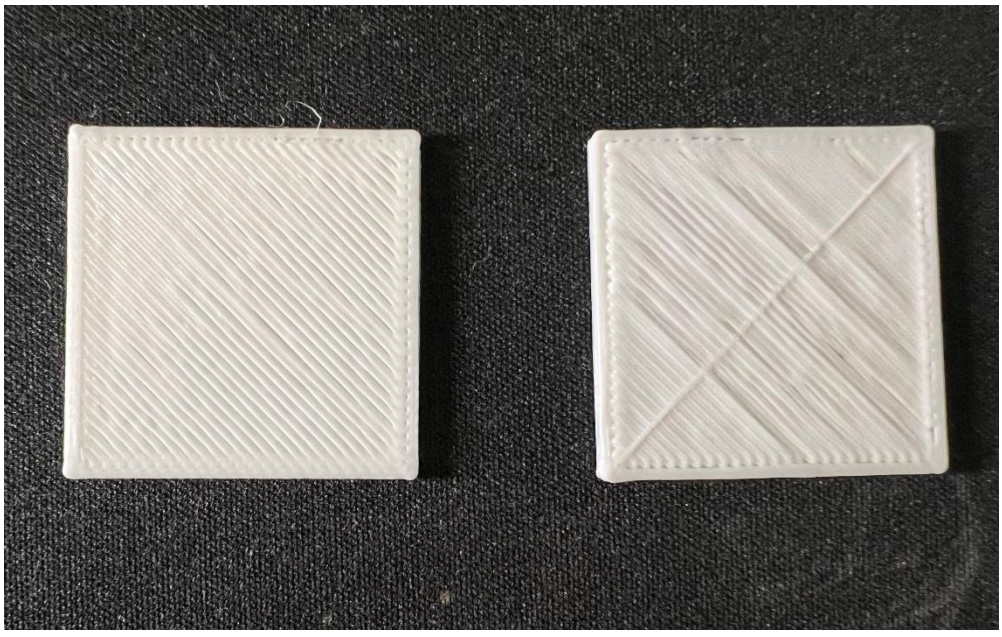

Figure 37 layer thickness of 0.4 and o.5 mm

	Table 4 - Layer Height (mm)				
	0.15	0.2	0.3	0.4	0.6
Side Length (mm)	30.13	30.14	29.98	30.16	30.20
	30.16	30.16	30.01	30.13	30.18
	30.14	30.13	29.96	30.20	30.17
	30.22	30.31	30.01	30.25	30.32
	30.25	30.25	30.05	30.21	30.36
	30.23	30.29	30.04	30.26	30.33
% Error	0.63%	0.71%	0.03%	0.67%	0.87%
Thickness (mm)	1.96	1.97	1.98	2.05	2.12
	1.99	1.99	1.97	2.06	2.15
	1.95	1.98	2.01	2.04	2.14
% Error	-1.67%	-1.00%	-0.67%	2.50%	6.83%
Surface roughness (µm)	17.88	13.06	23.58	24.73	20.39
	12.79	16.41	19.57	15.79	23.73
	19.51	5.81	18.7	25.51	15.65
	13.5	11.93	11.21	22.53	32.9
	19.94	18.01	18.81	23.11	27.36
Average	16.724	13.044	18.374	22.334	24.006

Figure 38 Table for different Layer height settings

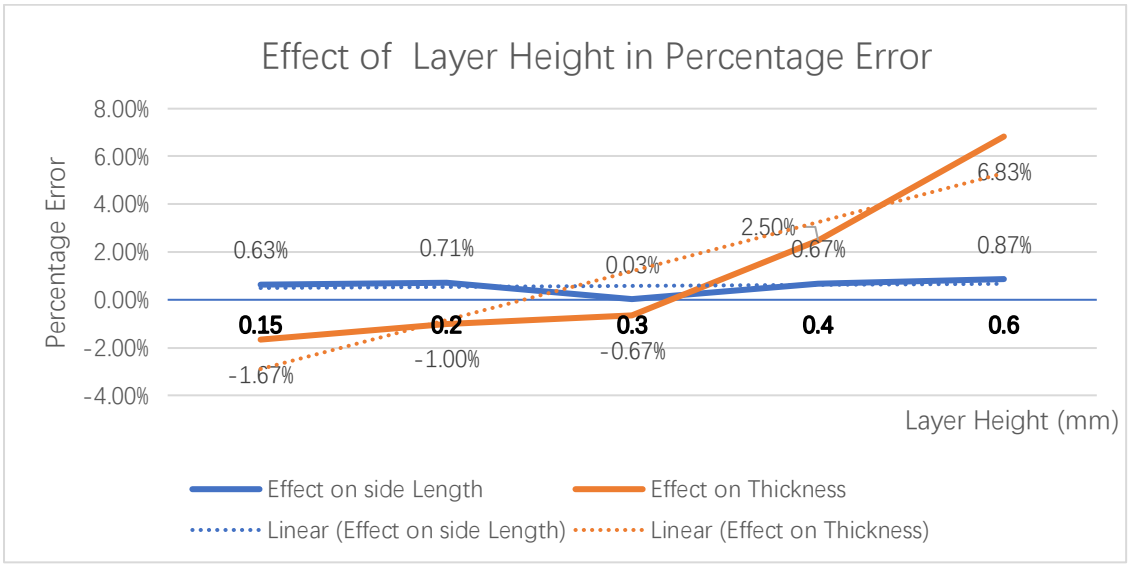

Figure 39 Effect of Layer Height for Percentage Error

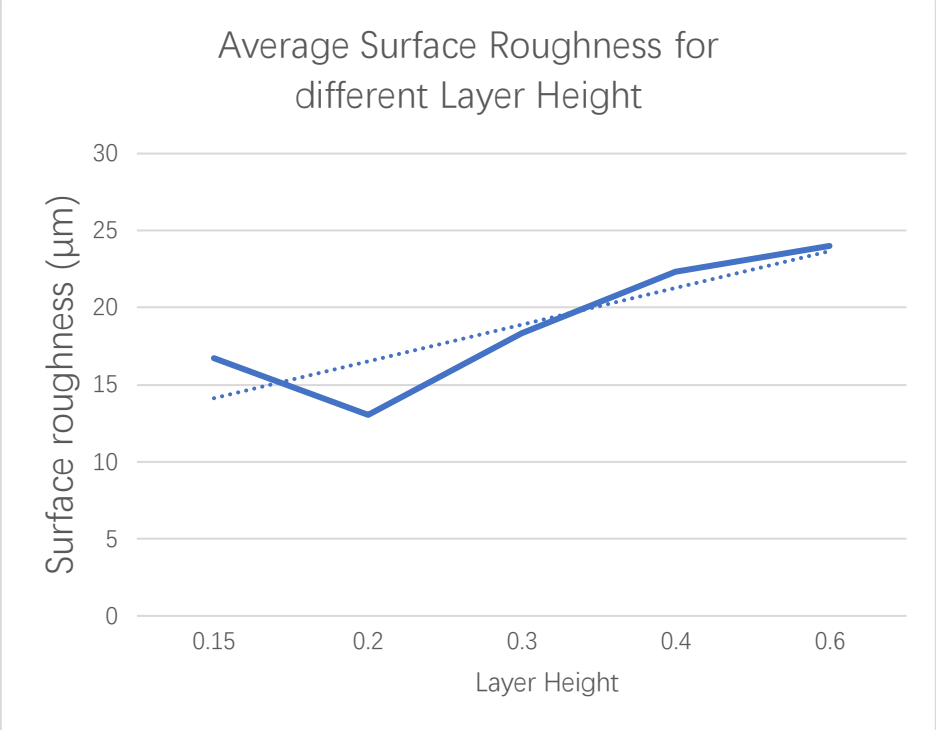

Figure 40 Effect of Layer Height on surface roughness

In general, higher Layer height would have larger percentage error and higher surface roughness.

5.1.5. Static Analysis

Linear regression model:

y ~ 1 + x1 + x2 + x3 + x4 + x1^2 + x2^2 + x3^2 + x4^2

Estimated Coefficients:

	Estimate	SE	tStat	pValue
(Intercept)	0.42794	0.24728	1.7306	0.11144
x1	-0.0042391	0.0024086	-1.76	0.10615
x2	-0.00035658	0.00030468	-1.1703	0.2666
x3	8.7645e-05	0.00015986	0.54826	0.59446
x4	-0.06344	0.039822	-1.5931	0.13945
x1^2	1.0798e-05	6.0166e-06	1.7947	0.1002
x2^2	3.3274e-06	1.5041e-06	2.2122	0.049034
x3^2	-2.5443e-07	8.4298e-07	-0.30183	0.76841
x4^2	0.092456	0.05067	1.8247	0.095301

Number of observations: 20, Error degrees of freedom: 11

Root Mean Squared Error: 0.00305

R-squared: 0.823, Adjusted R-Squared: 0.694

F-statistic vs. constant model: 6.4, p-value = 0.0031

5.2. For 5-axis Printing:

Figure 41 planar

Figure 42 Spiral toolpath

Figure 43 contour toolpath with 200 °C

Figure 44 Contour toolpath with 240 ℃

Figure 45 contour toolpath with 0.7 extrusion ratio

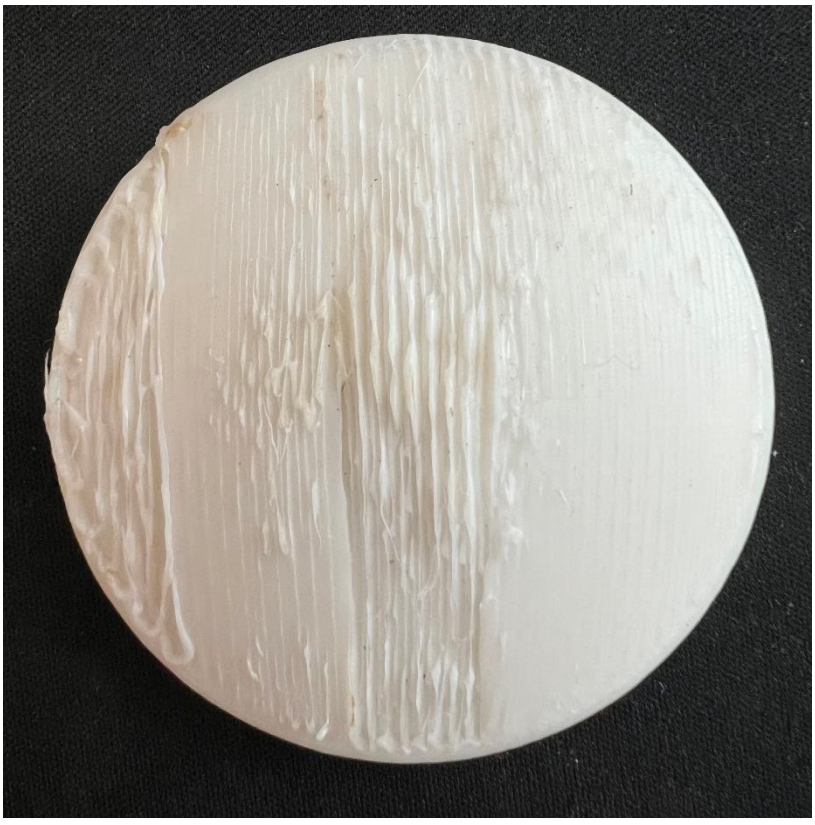

Figure 46 Zigzag toolpath

	Plannar		Contour				Zigzag		Spiral
	200°C		200°C		240°C		200°C		200°C
	24.37		10.24		10.22		7.94		6.47
	23.41		7.11		20.33		6.44		17.61
	28.55		7.61		7.98		33.64		16.74
	25.16		6.54		24.54		9.74		14.43
	9.99		19.04		28.13		10.91		15.93
Avg. (μm)	22.296		10.108		18.24		13.734		14.236

Figure 47 Average Surface Roughness for different settings

Similar trend as 3-axi 3D printing,

The Influence of Singularity is important for 5-axis printing.

6. Discussion

The results show the trends of:

• Printing at a lower temperature might reduces the error by improving accuracy, higher printing temperatures contribute to a greater positive error, possibly due to the filament spreading outwards.
• Faster printing speeds increase inaccuracy by causing lower accuracy during extrusion and placement of the filament.
• Increasing layer thickness leads to a sharp rise in error%. Thicker layers cause greater inaccuracy by spreading out more after extrusion.
• Thinner layers and lower printing speeds lead to negative errors, meaning the built part is smaller than the CAD design due to greater contraction.

For 5-axis printing:
Similar trends,
Patterns have more influence.
Effect of singularity.

Basically, the same results as literatures

Conflict between low temperature and high speed,

Limitation: not enough tests size to draw best prediction
More parameters could be considered like angles. etc.
More quality could be measured like strength.
Model shape could be more complex.

Future work: try to introduce the Neural network function.
Make a full factorial design.

7. Conclusion

• Printing at a lower temperature might reduces the error by improving accuracy, higher printing temperatures contribute to a greater positive error, possibly due to the filament spreading outwards.

• Faster printing speeds increase inaccuracy by causing lower accuracy during extrusion and placement of the filament.

• Increasing layer thickness leads to a sharp rise in error%., Thicker layers cause greater inaccuracy by spreading out more after extrusion.

• Thinner layers and lower printing speeds lead to negative errors, meaning the built part is smaller than the CAD design due to greater contraction.

8. References

Brion, D.A. and Pattinson, S.W. (2022) ‘Generalisable 3D printing error detection and correction via multi-head neural networks’, Nature communications, 13(1), pp. 1–14.

Chaidas, D. et al. (2016) ‘The impact of temperature changing on surface roughness of FFF process’, IOP Conference Series: Materials Science and Engineering, 161(1), p. 012033. Available at: https://doi.org/10.1088/1757-899X/161/1/012033.

Chohan, J.S. et al. (2022) ‘Optimization of FDM Printing Process Parameters on Surface Finish, Thickness, and Outer Dimension with ABS Polymer Specimens Using Taguchi Orthogonal Array and Genetic Algorithms’, Mathematical Problems in Engineering, 2022, p. e2698845. Available at: https://doi.org/10.1155/2022/2698845.

Dai, C. et al. (2018) ‘Support-free volume printing by multi-axis motion’, ACM Transactions on Graphics, 37(4), p. 134:1-134:14. Available at: https://doi.org/10.1145/3197517.3201342.

Ehsanul Haque, M. et al. (2019) ‘A Numerical Approach to Measure the Surface Roughness of FDM Build Part’, Materials Today: Proceedings, 18, pp. 5523–5529. Available at: https://doi.org/10.1016/j.matpr.2019.07.659.

Elkaseer, A., Schneider, S. and Scholz, S.G. (2020) ‘Experiment-Based Process Modeling and Optimization for High-Quality and Resource-Efficient FFF 3D Printing’, Applied Sciences, 10(8), p. 2899. Available at: https://doi.org/10.3390/app10082899.

Fang, G. et al. (2020) ‘Reinforced FDM: multi-axis filament alignment with controlled anisotropic strength’, ACM Transactions on Graphics, 39(6), p. 204:1-204:15. Available at: https://doi.org/10.1145/3414685.3417834.

Fernandes, J.F.M. (no date) ‘Study of the Influence of 3D Printing Parameters on the Mechanical Properties of PLA’.

Gao, W. et al. (2015) ‘The status, challenges, and future of additive manufacturing in engineering’, Computer-Aided Design, 69, pp. 65–89. Available at: https://doi.org/10.1016/j.cad.2015.04.001.

Griffiths, C.A. et al. (2016) ‘A design of experiments approach for the optimisation of energy and waste during the production of parts manufactured by 3D printing’, Journal of Cleaner Production, 139, pp. 74–85. Available at: https://doi.org/10.1016/j.jclepro.2016.07.182.

Hada, T. et al. (2020) ‘Effect of Printing Direction on the Accuracy of 3D-Printed Dentures Using Stereolithography Technology’, Materials, 13(15), p. 3405. Available at: https://doi.org/10.3390/ma13153405.

Hong, F. et al. (2022) ‘Open5x: Accessible 5-axis 3D printing and conformal slicing’, in Extended Abstracts of the 2022 CHI Conference on Human Factors in Computing

Systems. New York, NY, USA: Association for Computing Machinery (CHI EA '22), pp. 1–6. Available at: https://doi.org/10.1145/3491101.3519782.

Huang, Y. et al. (2015) 'Additive Manufacturing: Current State, Future Potential, Gaps and Needs, and Recommendations', Journal of Manufacturing Science and Engineering, 137(1). Available at: https://doi.org/10.1115/1.4028725.

Isa, M.A. and Lazoglu, I. (2019) 'Five-axis additive manufacturing of freeform models through buildup of transition layers', Journal of Manufacturing Systems, 50, pp. 69–80.

Jin, Y. et al. (2015) 'Quantitative analysis of surface profile in fused deposition modelling', Additive Manufacturing, 8, pp. 142–148. Available at: https://doi.org/10.1016/j.addma.2015.10.001.

Jin, Y. et al. (2017) 'Modeling and process planning for curved layer fused deposition', The International Journal of Advanced Manufacturing Technology, 91(1), pp. 273–285. Available at: https://doi.org/10.1007/s00170-016-9743-5.

Lalehpour, A. and Barari, A. (2016) 'Post processing for Fused Deposition Modeling Parts with Acetone Vapour Bath', IFAC-PapersOnLine, 49(31), pp. 42–48. Available at: https://doi.org/10.1016/j.ifacol.2016.12.159.

Matsuzaki, R. et al. (2016) 'Three-dimensional printing of continuous-fiber composites by in-nozzle impregnation', Scientific Reports, 6(1), p. 23058. Available at: https://doi.org/10.1038/srep23058.

Pérez, M. et al. (2018) 'Surface Quality Enhancement of Fused Deposition Modeling (FDM) Printed Samples Based on the Selection of Critical Printing Parameters', Materials, 11(8), p. 1382. Available at: https://doi.org/10.3390/ma11081382.

Popescu, D. et al. (2018) 'FDM process parameters influence over the mechanical properties of polymer specimens: A review', Polymer Testing, 69, pp. 157–166.

Santana, L., Alves, J.L. and Netto, A. da C.S. (2017) 'A study of parametric calibration for low cost 3D printing: Seeking improvement in dimensional quality', Materials & Design, 135, pp. 159–172.

Singamneni, S. et al. (2012) 'Modeling and evaluation of curved layer fused deposition', Journal of Materials Processing Technology, 212(1), pp. 27–35. Available at: https://doi.org/10.1016/j.jmatprotec.2011.08.001.

Valerga, A.P. et al. (2018) 'Influence of PLA Filament Conditions on Characteristics of FDM Parts', Materials, 11(8), p. 1322. Available at: https://doi.org/10.3390/ma11081322.

Valerga, A.P. et al. (2019) 'Impact of Chemical Post-Processing in Fused Deposition Modelling (FDM) on Polylactic Acid (PLA) Surface Quality and Structure', Polymers, 11(3), p. 566. Available at: https://doi.org/10.3390/polym11030566.

Wang, M. et al. (2019) ‘Research and implementation of a non-supporting 3D printing method based on 5-axis dynamic slice algorithm’, Robotics and Computer-Integrated Manufacturing, 57, pp. 496–505.

Wulle, F. et al. (2017) ‘Workpiece and Machine Design in Additive Manufacturing for Multi-Axis Fused Deposition Modeling’, Procedia CIRP, 60, pp. 229–234. Available at: https://doi.org/10.1016/j.procir.2017.01.046.

Wüthrich, M. et al. (2020) ‘Novel 4-Axis 3D Printing Process to Print Overhangs without Support Material’, in International Conference on Additive Manufacturing in Products and Applications. Springer, pp. 130–145.

Yang, L. et al. (2019) ‘Experimental Investigations for Optimizing the Extrusion Parameters on FDM PLA Printed Parts’, Journal of Materials Engineering and Performance, 28(1), pp. 169–182. Available at: https://doi.org/10.1007/s11665-018-3784-x.

Yao, Y. et al. (2021) ‘3D Printing of Objects with Continuous Spatial Paths by a Multi-Axis Robotic FFF Platform’, Applied Sciences, 11(11), p. 4825. Available at: https://doi.org/10.3390/app11114825.

Zhang, T. et al. (2021) ‘Singularity-Aware Motion Planning for Multi-Axis Additive Manufacturing’, IEEE Robotics and Automation Letters, 6(4), pp. 6172–6179. Available at: https://doi.org/10.1109/LRA.2021.3091109.

9. Appendix: A (not complete yet)

Initial plan:

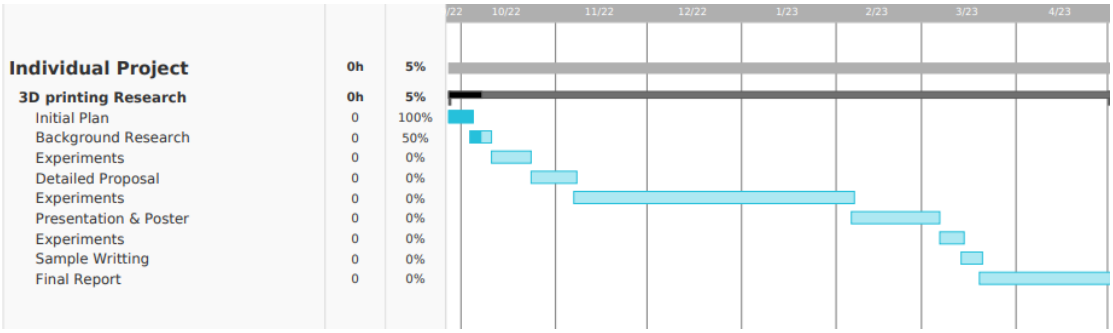

Proposal:

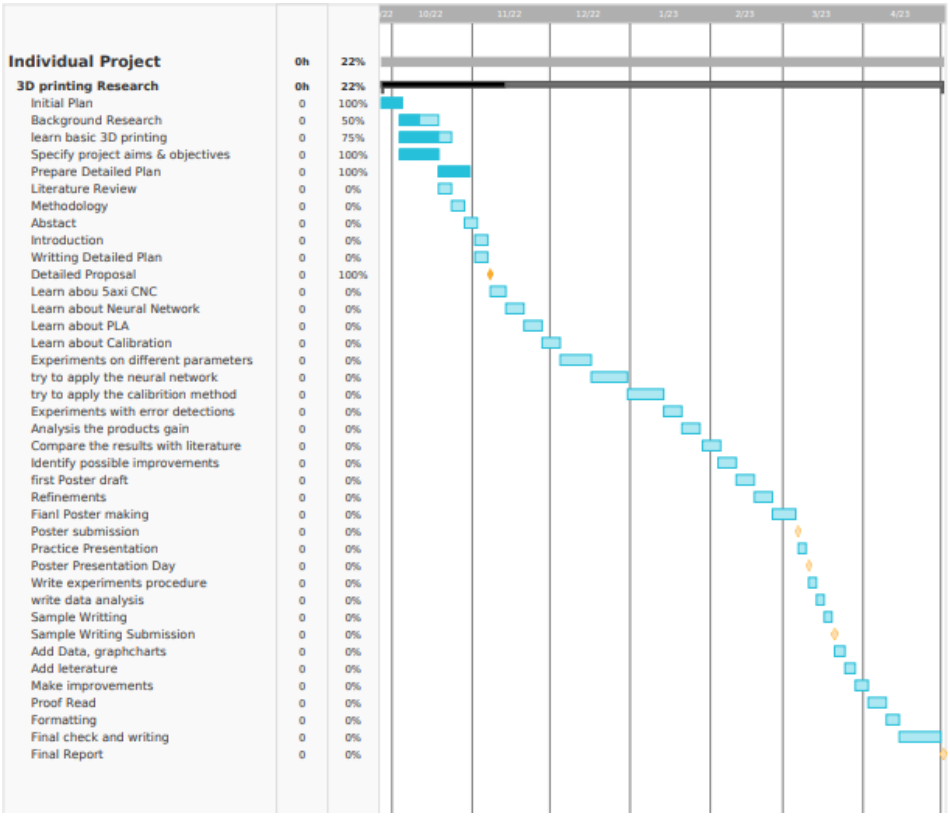

Reflection: should arrange experiments more actively,

Should conduct with supervisor and assistance more frequently.

Should consider more for the lack availability of the equipment.